Asian Journal of Control, Vol. 16, No. 1, pp. 117–125, January 2014
Published online 27 September 2012 in Wiley Online Library (wileyonlinelibrary.com) DOI: 10.1002/asjc.599

KNOWLEDGE-BASED EXPERT CONTROL OF THALAMIC NEURON FIRING MODE

Christ Devia, Manuel A. Duarte-Mermoud, and María de la Luz Aylwin O.

ABSTRACT

This work sheds light on the possibility of using control strategies to set the parameters of electric stimulation, a commonly used technique in severe human central nervous system diseases. Currently, parameters of electric stimulation are set through a trial and error process, with a lot of undesirable side effects. Accordingly, and based on the problem of having a population of sick neurons embedded in a population of normal neurons, this work explores the possibility of using a control system based on the behavior of healthy neurons to set current parameters able to modify the electric behavior of sick neurons. Specifically, we posit a knowledge-based expert control system that modifies the firing mode of a thalamic neuron by applying a control stimulation current, with the aim of making it fire in the same mode as a reference thalamic neuron. The controller parameters are tuned based on some characteristics of neurons that have to be determined through experiments before their application, but this controller does not require a detailed mathematical model of each neuron. Simulation results indicate that the proposed system satisfies the control objectives.

Key Words: Thalamic neuron model, neuron input current estimator, expert control system, neuron control.

I. INTRODUCTION

Currently three main therapies are used to stimulate the human nervous system. These are deep brain stimulation (DBS), vagus nerve stimulation, and transcranial magnetic stimulation. Even though they are successful therapies for many diseases, tough questions remain concerning their action mechanism at the cellular level, as well as ethical challenges [1, 2].

Examples of central nervous system diseases—mainly movement disorders and neuropsychiatric diseases such as Parkinson's disease, essential tremor, dystonia, obsessive-compulsive disorder, depression, Tourette's syndrome, epilepsy, minimally conscious state, and headaches—can be relieved by DBS therapies [4, 5]. Deep brain stimulation therapy delivers a current through electrodes inserted in the brain with an apparatus similar to a cardiac pacemaker, with the main target subcortical structures such as the cerebellum, thalamic nuclei, and basal ganglia system [3]. The electrode performs extracellular stimulation of surrounding brain tissues, diminishing the symptoms of movement disorders [6]. Currently more than 75,000 patients worldwide have a stimulator device implanted [1, 4].

The surgical procedure to implant DBS electrodes includes testing the stimulation during surgery with an awake patient in order to have spoken feedback of any undesired side-effects [7–11]. In DBS a wide volume of neurons is stimulated, which in many cases is greater than the area of interest [12, 13], and stimulation is delivered constantly without any feedback of actual changes in brain activity [1, 4]. These limitations pose the necessity of developing intelligent closed-loop DBS devices, as stated by Shah *et al*. [1].

This work presents the possibility of using a control strategy to set the parameters of electric stimulation including a feedback stage. To do this we simulated a system of two thalamic neurons; one is the reference neuron, whose pattern of electrical activity we want to reproduce in the other neuron, called the sick neuron, that is, the neuron whose behavior we want to modify assuming it has diseased behavior. Both were simulated through an integrate-and-fire-or-burst (IFB) model, which reproduced the behavior of a neuron from the thalamic lateral geniculate nucleus. The proposed control system designs the control current delivered to the sick neuron based on the identification of the firing pattern of both neurons. The simulated system was developed based on three main assumptions that will be discussed further in the conclusions. The assumptions are: (i) only membrane potential would be available for measurement on each neuron; (ii) the control action would be applied only to the sick neuron; and (iii) there would still be normal neurons in the brain that could perform the role of the reference neuron.

Manuscript received October 29, 2010; revised February 23, 2012; accepted May 14, 2012.

Christ Devia and Manuel A. Duarte-Mermoud (corresponding author, e-mail: mduartem@ing.uchile.cl) are with Department of Electrical Engineering, University of Chile, Av. Tupper 2007, Casilla 412-3, Santiago, Chile.

María de la Luz Aylwin O. is with the Program of Physiology and Biophysics, ICBM, University of Chile, Av. Independencia 234, Santiago, Chile.

The work reported here has been supported by CONICYT-CHILE through grant FONDECYT No. 1061170. It was also supported by Iniciativa Científica Milenio ICM P04-068-F.

This article is divided into five sections. Besides the introductory Section I, Section II deals with the model IFB used to describe the neurons. In Section III the proposed control scheme is presented in detail. Section IV is devoted to the study of the proposed control system, presenting some simulations. Finally, some conclusions are drawn in the fifth section.

II. IFB MODEL

The integrate-and-fire-or-burst (IFB) system is based on Labique's classic model, integrate-and-fire [14]. The IFB model was proposed in 2000 by Smith *et al*. [15] and was tuned to reproduce the firing mode of neurons from the thalamic lateral geniculate nuclei of young cats. The parameters used in the model were established to reproduce the main features of these thalamic neurons [16], such as tonic firing (see Fig. 1a), and rebound burst mode (see Fig. 1b). This model depends on two different thresholds, $V_{h,}$ responsible for the activation of the burst spiking mode, and V_θ, responsible for the activation of tonic firing. These thresholds were measured intracellularly by Smith *et al*. for young cats (See Table I). The model describes the dynamic of membrane voltage V_m through three equations, (1.1)–(1.3). At time t, and based on the V_m value at time t^-, previous to t, as follows:

$$If \quad V_m(t^-) < V_\theta \Rightarrow C\frac{dV_m(t)}{dt} = I_{IN} - I_L - I_T \tag{1.1}$$

$$If \quad V_m(t^-) = V_\theta \Rightarrow V_m(t) = V_{spike} \tag{1.2}$$

$$If \quad V_m(t^-) = V_{spike} \Rightarrow V_m(t) = V_{reset} \tag{1.3}$$

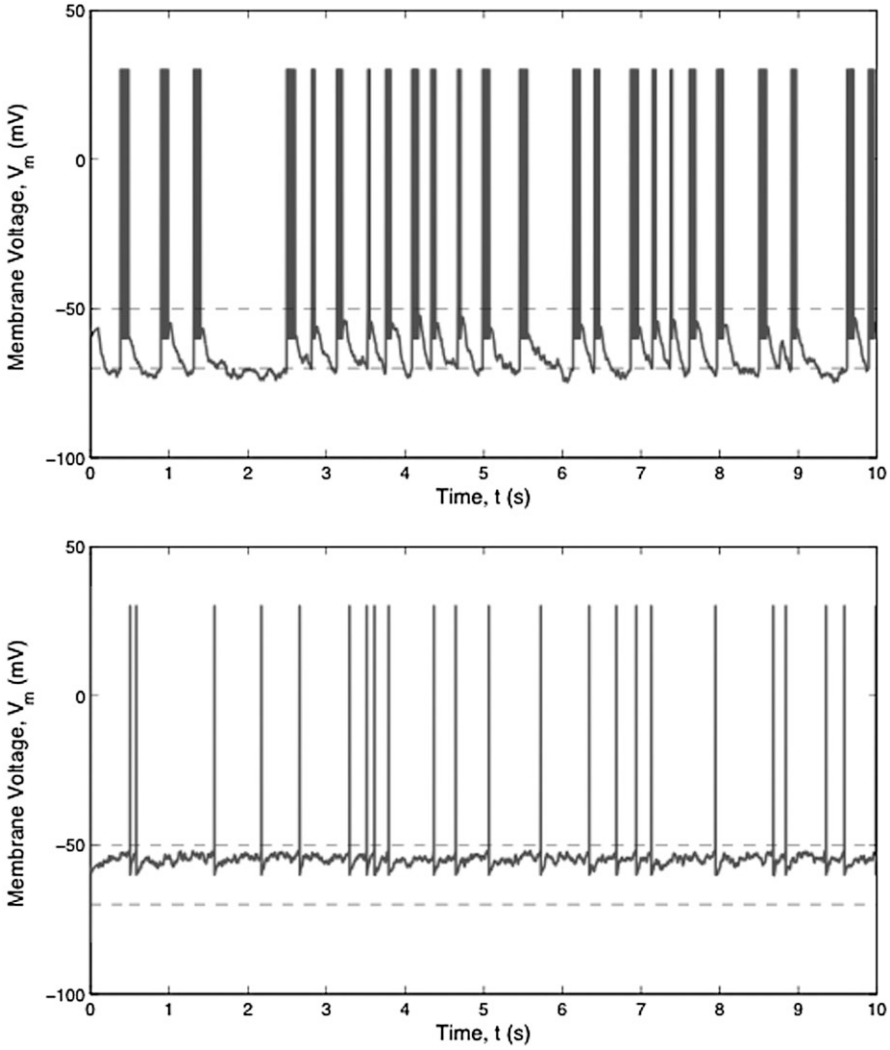

Fig. 1. Examples of IFB model membrane voltage due to simulated synaptic current. Left: Burst firing, mean value $I_{IN} = 152.0$ (nA). Right: Tonic firing, mean value $I_{IN} = 738.4$ (nA).

Table I. IFB Model Parameters [13].

Parameter	Value	Unit	Parameter	Value	Unit
V_θ	−50	mV	g_L	0.035	mS/cm^2
V_h	−70	mV	g_T	0.8	mS/cm^2
V_{reset}	−60	mV	τ_h^+	100	ms
V_{spike}	30	mV	τ_h^-	20	ms
V_L	−75	mV	C	2	μF/cm^2
V_T	120	mV			

V_m : Neuron membrane voltage or membrane potential.
V_θ : Threshold voltage over which an action potential is triggered.
V_{reset} : Maximum voltage reached by an action potential.
V_{reset} : Rest voltage reached after an action potential.
I_{IN} : Total current that stimulates the neuron (*i.e.* synaptic current).
C : Membrane capacitance

The differential equation (1.1) is solved every time membrane voltage V_m is lower than threshold voltage V_θ. Equation (1.2) sets membrane voltage V_m to V_{spike}, immediately after threshold voltage V_θ is reached. On the other side, Equation (1.3) sets membrane voltage V_m to V_{reset} immediately after an action potential occurs. The dynamic of $V_m\ (t)$ at each instant depends on membrane voltage at the time immediately before, called $V_m\ (t^-)$. Table I shows the parameter values used for the model in all simulations done in this study, which correspond with the thalamic lateral geniculate nuclei of young cats [15]. The currents of leak conductance due to movement of low-threshold Ca^{++} ions, I_L and I_T, are given by:

$$I_L = g_L(V_m(t) - V_L) \tag{2}$$

$$I_T = g_T m_\infty h(V_m(t) - V_T) \tag{3}$$

Low-threshold Ca^{++} current depends also on the characterization of its activation denoted as m_∞, given by (4), and of its inactivation denoted as h, given by (5).

$$m_\infty = \begin{cases} 1 & V_m(t) - V_h \geq 0 \\ 0 & V_m(t) - V_h < 0 \end{cases} \tag{4}$$

$$\dot{h} = \begin{cases} \dfrac{-h}{\tau_h^-} & V_m(t) - V_h \geq 0 \\ \dfrac{(1-h)}{\tau_h^+} & V_m(t) - V_h < 0 \end{cases} \tag{5}$$

V_h is the threshold voltage under which a rebound burst is triggered. The parameter τ_h^+ represents the duration of the burst, and τ_h^- indicates the duration of the hyperpolarization necessary to recruit a maximal post-inhibitory rebound response.

The input current I_{IN} applied to neurons was produced based on a model of synaptic current which represents the afferent current (also called stimulus current) due to synaptic interaction with other neurons in the same neural circuit. It was modeled as a sum of exponential functions that follow independent Poisson processes [17, 18]. Because of the stochastic nature of this model of synaptic currents, it is not possible to find two identical processes. These currents drive neurons to fire in tonic mode (TM) or burst mode (BM), both at irregular frequencies just like what happens in a real neuron. (See Fig. 1).

III. CONTROL STRATEGY

As stated in the previous section, the idea of the control system is to change or to maintain the firing mode of the sick neuron in order to make it fire in reference neuron mode, through the application of a suitable control current, I_c. This control current is designed based only on knowledge of the membrane voltage, V_m of the neurons (see Fig. 2).

As seen in Fig. 2, the controller receives as inputs V_m of both neurons, at least 500 ms of membrane voltage data V_m from each neuron, and from these values determines the firing mode of each neuron, estimates input current for each neuron, and then computes the control action. In this way, the control system developed here is a closed-loop knowledge-based reference control. An expert system was chosen instead of a classical control system for one main reason; in real applications it is difficult to develop an accurate mathematical model of each neuron to be controlled, which is why the control system developed here is based only on: (i) V_m measurement; and (ii) the knowledge of V_θ and V_h and the parameters of (6) and (7), all of which can be determined through laboratory experiments [19, 20].

The control current is defined as $I_c = \tilde{I}_{RN} - \tilde{I}_{SN}$, where the currents $\tilde{I}_{RN}$ and $\tilde{I}_{SN}$ are estimations of afferent current to the reference and sick neuron, respectively. In order to calculate I_c and for the sake of clarity, the control system was divided into three blocks, as seen in Fig. 2. The first block, called Classification Rules, identifies the firing mode (burst or tonic) of both neurons. The second block, called the Current Estimator, estimates the input current at the entry of each neuron. The third block, called Control Action, computes the control current I_c.

3.1 Classification rules

In order to classify the firing mode of a neuron, enough information must be available to ensure good performance of the control system, which is why this block classifies the firing mode of a neuron only after 500 milliseconds of simulation. From these 500-length voltage vectors the classifier identifies the firing mode of each neuron. This is done

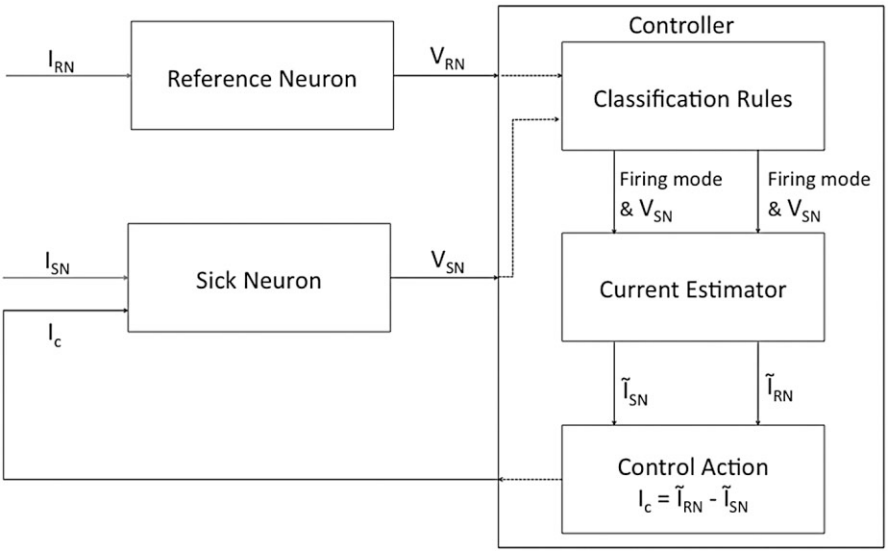

Fig. 2. Diagram of the control scheme and neuron inputs and outputs.

verifying that each component of voltage vector V_m (i) is within one of these constraints:

1. If at least one component $V_m(i) \leq V_h$, then the neuron is classified as firing in BM.
2. If at least one component $V_m(i) \geq V_\theta$, and all components are $V_m(i) > V_h$, then the neuron is firing in TM.
3. If all vector components satisfy $V_h < V_m(i) < V_\theta$ then the neuron is at rest, also called the passive mode, where no spike occurs.

3.2 Current estimator

The relationship between neuron firing frequency, measured from membrane voltage signal V_m, and the neuron stimulus amplitude I_{IN}, was studied from the IFB model. The stimulus applied was a square wave signal of fixed width and variable amplitude in the range –2 μA to 2 μA. There were differences in mean frequency of membrane voltage between TM and BM. In burst firing, the mean frequency was over 3 KHz, whereas in tonic firing, frequency was never over 0.3 KHz. Based on this data, two different estimators were developed, one for the BM, and the other for the TM.

For the TM a quadratic relationship, equation (6), between the stimulus amplitude I_{IN} and the spike frequency of membrane voltage signal V_m was determined from linear regressions of discharge data collected through simulations. (See Fig. 3). This equation allows us to estimate the current of stimulus $\tilde{I}_{TM}$ from the mean frequency of membrane voltage signal f_m measured over V_m.

$$\tilde{I}_{TM} = 40.2 f_m^2 + 16.85 f_m + 0.67 \quad (6)$$

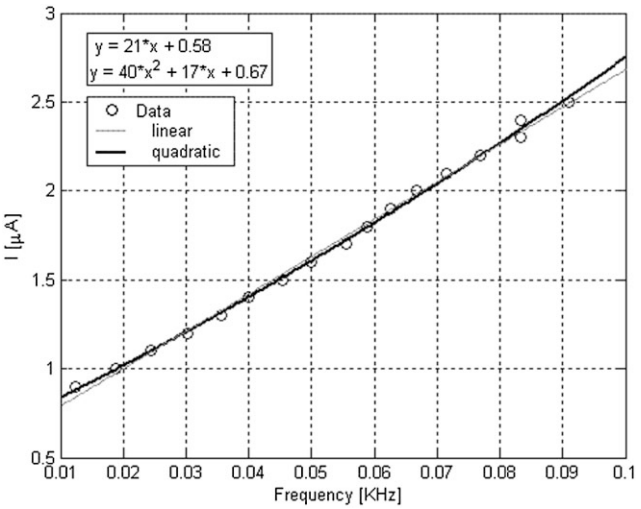

Fig. 3. Stimulus amplitude versus spike frequency of membrane voltage for the tonic mode.

For BM it was not possible to define a current estimator based on V_m spike frequency. Even though the relationship between $\tilde{I}_{BM}$ and f_m was linear, the slope was small in magnitude generating important numerical errors; and the literature lacks a consensus on deciding if a neuron is firing in BM or TM from a single spike. Considering these reasons and the fact that thalamic neurons show rebound burst that comes only after hyperpolarization of membrane voltage V_m below threshold voltage V_h, the current estimator for burst firing was built based on the derivative of membrane voltage vector $\dot{V}_m$. A linear relationship was found between the hyperpolarization voltage slope generated and the maximum amplitude of the applied stimulus, as seen in Fig. 4.

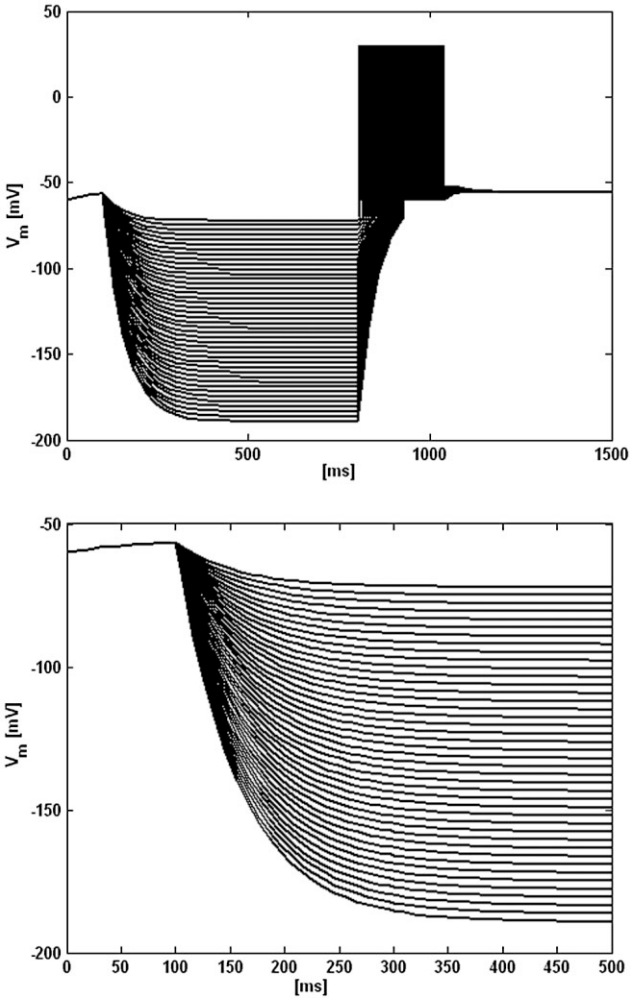

Fig. 4. (a) Rebound burst for different stimulus amplitudes. (b) Zoom of voltage slope before rebound between 0 and 500 ms.

In Fig. 5 the relationship between the derivative $\dot{V}_m$ near –0.25 mV/s, and the stimulus amplitude is shown. Equation (7), obtained from linear regressions of discharge data collected through simulations, was used to estimate I_{BM} (see Fig. 5).

$$\tilde{I}_{BM} = 2\dot{V}_m + 0.6 \tag{7}$$

IV. SIMULATION RESULTS

The control system proposed in the previous section was applied in two different cases. First, when input current to neurons was a square pulse, and second when it was a Poisson process. As a first test the reference neuron was in BM, stimulated with square pulse from 0.3 μA to 0.1 μA which is the hyperpolarized stage. This current was estimated as having $\tilde{I}_{RN} = 0.0949(\mu A)$. The sick neuron was

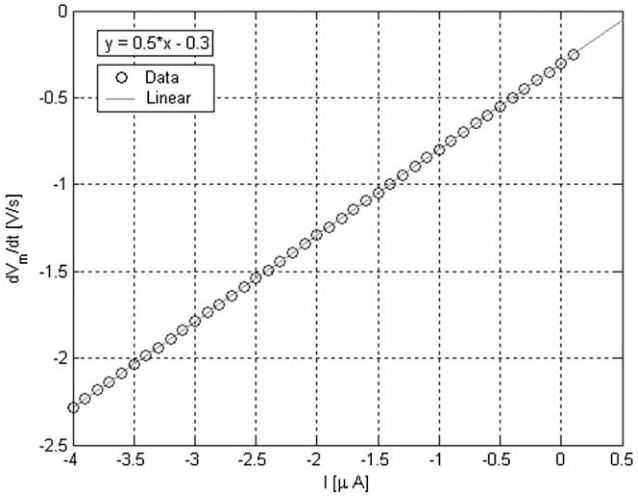

Fig. 5. Relationship between $\dot{V}_m$ and stimulus amplitude in BM.

stimulated with a constant 0.9 μA, which was estimated as $\tilde{I}_{SN} = 1.0467(\mu A)$. Fig. 6 shows the control applied to the sick neuron firing initially in TM, then when applying the control current at t =500 ms, it starts to respond in BM, like the reference neuron.

Fig. 7 presents the case in which the reference neuron is firing in TM, and the sick neuron is initially responding in BM. When the control current is applied at 500 ms, the sick neuron starts responding in TM. In this case the current of the reference neuron was 1.1 μA, estimated as $\tilde{I}_{RN} = 1.1049(\mu A)$, and had a square pulse between 0.3 μA and –0.1 μA, the last value responsible for hyperpolarization of the sick neuron. The input current was estimated as $\tilde{I}_{SN} = 0.1879(\mu A)$. The average discharge of the sick neuron was $f_m = 20$ Hz, compared with 24 Hz for the reference neuron.

Figs 8 and 9 show the results of applying the control system when a Poisson process generating stimulus current is used. Fig. 9 shows the case when the sick neuron is responding in TM, but once the current control is applied at t = 500 ms, starts responding in BM. The mean component of the Sick Neuron stimulus current was 1.0382 μA and 0.1206 μA for the reference neuron. These values were estimated as $\tilde{I}_{SN} = 1.1790(\mu A)$, and $\tilde{I}_{RN} = -0.6441(\mu A)$, respectively.

Fig. 9 shows the successful control of a burst type discharge. For the sick neuron the stimulus has a constant mean value of 0.0812 μA, which was estimated as $\tilde{I}_{SN} = 0.0340(\mu A)$. For the reference neuron, the mean of the applied current was 1.0395 μA and was estimated as $\tilde{I}_{RN} = 1.0212(\mu A)$. These estimation errors in turn produce differences in the frequency discharge of each neuron, with the reference neuron discharging at 21 Hz, and the sick neuron discharging at 16 Hz.

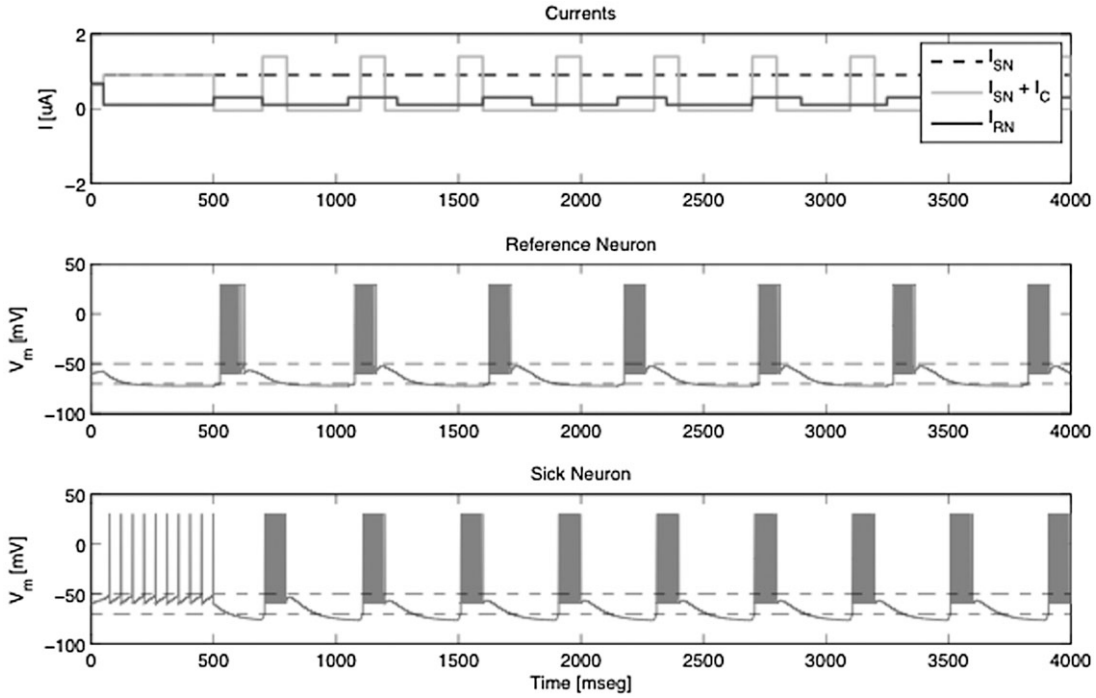

Fig. 6. TM control using noiseless stimulus current. Upper: Stimulus applied to each neuron. Center: Membrane voltage of the reference neuron in BM. Lower: Membrane voltage of the sick neuron, in TM until 500 ms when *Ic* was applied.

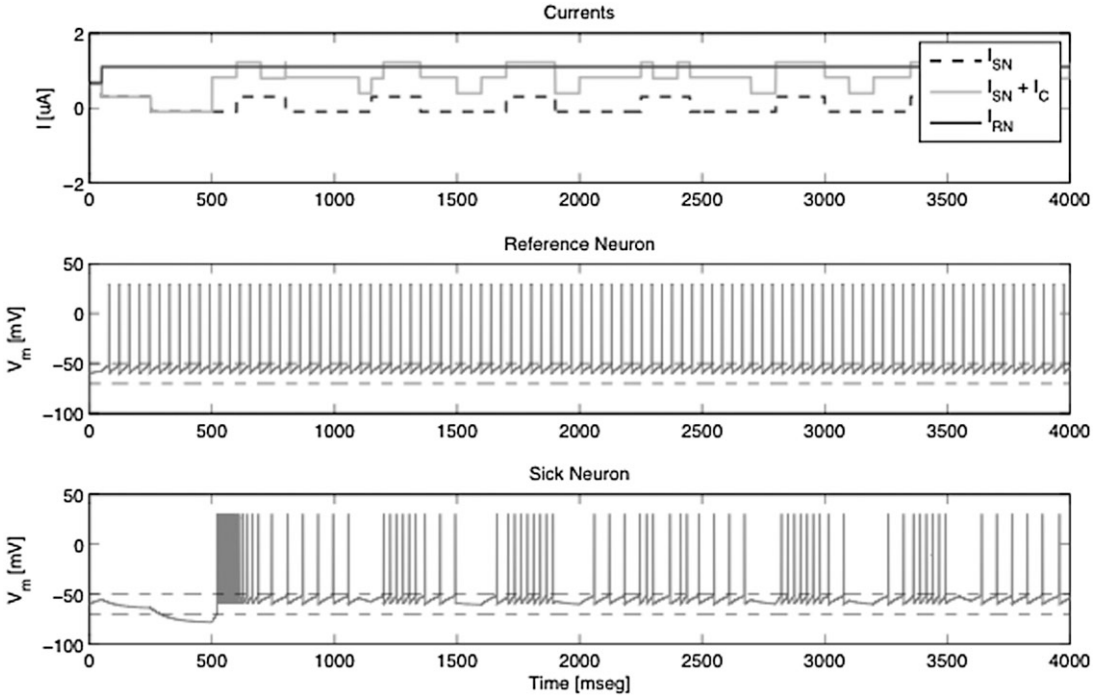

Fig. 7. Burst mode control using noiseless current. Upper: Stimulus applied to each neuron. Center: Membrane voltage of the reference neuron in TM. Lower: Membrane voltage of the sick neuron, in BM until 500 ms.

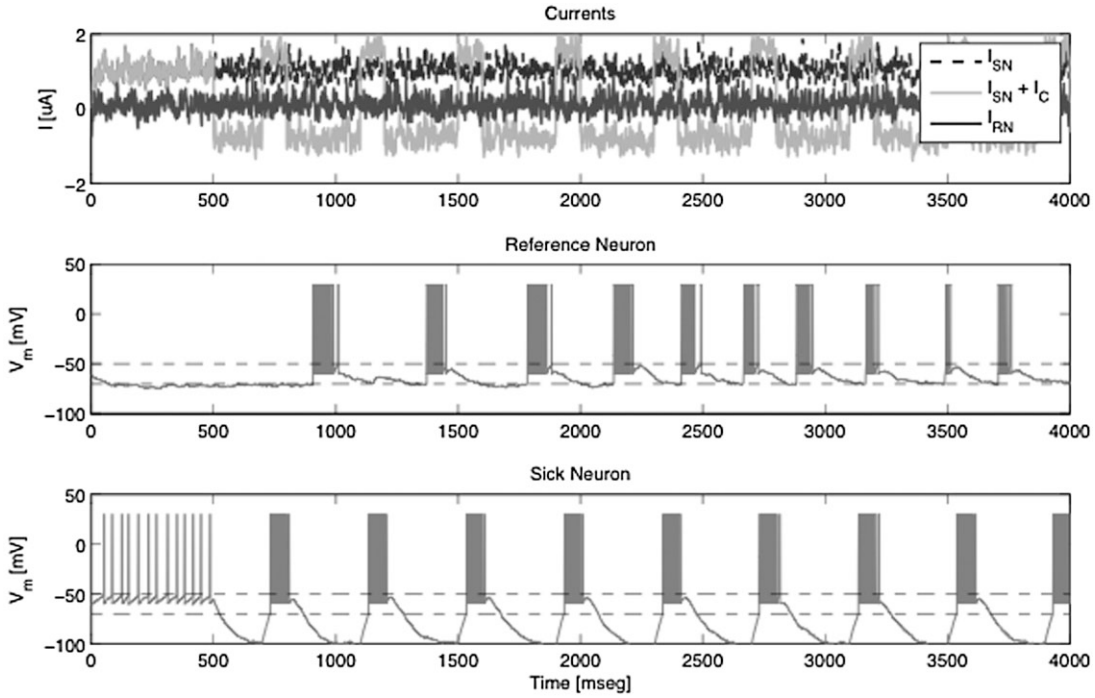

Fig. 8. Tonic Mode Control using SSC. Upper: Stimulus applied to each neuron. Center: Membrane voltage of the reference neuron in BM. Lower: Membrane voltage of the sick neuron in TM until 500 ms.

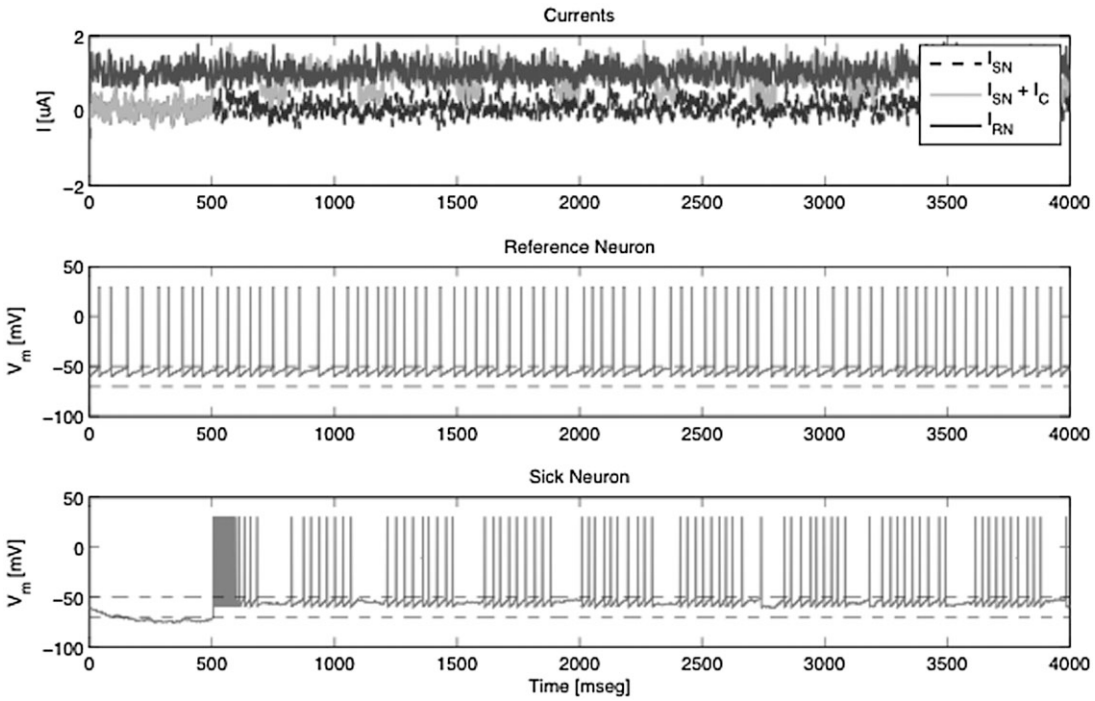

Fig. 9. BM control. Upper: Stimulus applied to each neuron. Center: Membrane voltage of the reference neuron in TM. Lower: Membrane voltage of the sick neuron, in BM until 500 ms.

Table II. Estimation errors for TM and BM.

Mean Value	Estimation	Error	Mode-Stimulus
0.9	0.8842	1.75%	*Tonic – constant*
1.1	1.1049	0.44%	*Tonic – constant*
1.0339	1.0810	4.55%	*Tonic – SSC*
1.0998	1.0684	2.85%	*Tonic – SSC*
Average error: 2.39%; Standard deviation: 1.74%			
0.1	0.0949	5.1%	*Burst – constant*
−0.1	−0.1034	3.4%	*Burst – constant*
0.1439	0.0736	48.8%	*Burst – SSC*
0.15	−0.1852	223.46%	*Burst – SSC*
Average error: 7.29%; Standard deviation: 104.31%			

Based on these results, it can be seen that the control objective was reached in all cases since the response mode of the sick neuron was modified in order to achieve the mode imposed by the reference neuron. The current estimation errors vary according to whether the estimation is done in TM or BM. Table II shows the percentage of error obtained in the four cases presented above. The estimation error was computed as the quotient between the estimated and true values of the current applied, expressed as a percentage as shown in (8).

$$e = \left| \frac{\tilde{I}}{I} - 1 \right| \cdot 100 \tag{8}$$

The cases shown in Figs 6 and 7 are instances in which the stimulus currents are noiseless and take constant values. The average estimation error in TM is 1.95%, whereas in BM it was 4.25%. In the cases shown in Figs 8 and 9, when the stimuli are generated by means of a Poisson process, the average estimation error was 3.7% in TM and 136.13% in BM. Therefore, it can be concluded that the estimation block is robust for TM, and less accurate for BM especially when a Poisson process is used as input current. This problem is mainly due to the fact that the estimator block in TM uses the mean value of the discharge frequency of the vector voltage, which makes it more immune to noise than in BM where the estimation is based on only one point of the vector voltage, and then is highly dependent on the noise present at that chosen point.

Robustness of the control system is considered in our study as we have analyzed the cases of deterministic and stochastic input currents. Furthermore, in general, the dynamic responses of neurons within the physiological ranges are restricted. So we do not expect major changes in the dynamics studied here when parameters variations occur. This has been observed in several simulations performed by us, but not reported here for the sake of space.

V. CONCLUSIONS

A firing-mode control system based only on neuron membrane voltage was designed and applied. Using its knowledge of some neuron characteristics, the control system is able to identify the neuron-firing mode and to determine the control current necessary to apply so that the firing mode of the sick /neuron is changed to that of the reference neuron.

By applying this control scheme to neurons stimulated by square wave current signals and Poisson stimulus current, it was verified that the estimation block is more accurate in TM than in BM since it is based on an average value, being less sensitive to noise on the membrane voltage signals. This problem could be solved by reformulating the estimation block in BM considering the variance of the information rather than using only one point. Work is currently underway to improve this aspect of the controller.

The proposed control system assumes that intracellular voltage is available (to be measured), as well as the possibility of stimulating only one neuron. These assumptions were quite unrealistic some time ago, but may become possible in the near future using nanolectrodes [21]. Yu *et al*. [22] have been able to measure and stimulate the membrane voltage in the same neuron, which opens the possibility that control strategies, such as the one proposed here, could be implemented *in vivo*, stimulating specific neurons and avoiding affecting healthy tissue in the neighboring areas, as occurs with DBS at present.

Finally, as pointed out by one reviewer, the proposed control contains a closed-loop stage and in that sense, stability issues associated to this problem should be addressed as future work.

REFERENCES

1. Shah, R. S., S. Chang, H. Min, Z. Cho, C. D. Blaha, and K. H. Lee, "Deep Brain Stimulation: Technology at the cutting edge," *J. Clin. Neurol.*, Vol. 6, No. 4, pp. 167–182 (2010).
2. Bell, E., G. Mathieu, and E. Racine, "Preparing the ethical future of deep brain stimulation," *Surg. Neurol.*, Vol. 72, No. 6, pp. 577–586 (2009).
3. Kahane, P. and A. Depaulis, "Deep brain stimulation in epilepsy: what is next?" *Curr. Opin. Neurol.*, Vol. 23, No. 2, pp. 177–182, April (2010).
4. Abbott, A., "Deep in thought," *Nature*, Vol. 436, pp. 18–19 (2005).
5. Anderson, W. S. and F. A. Lenz, "Surgery insight: Deep brain stimulation for movement disorders," *Nature Clin. Prac. Neurol.*, Vol. 2, No. 6, pp. 310–320 (2006).
6. Montgomery, E. B. and J. T. Gale, "Mechanisms of action of deep brain stimulation (DBS)," *Neurosci. Biobehav. Rev.*, Vol. 32, pp. 388–407 (2008).

7. Hariz, G. M., M. Lindberg, and A. T. Bergenheim, "Impact of thalamic deep brain stimulation on disability and health-related quality of life in patients with essential tremor," *J. Neurol. Neurosurg. Psych.*, Vol. 72, pp. 47–52 (2002).
8. Saint-Cyr, J. A., L. L. Trépanier, R. Kumar, A. M. Lozano, and A. E. Lang, "Neuropsychological consequences of chronic bilateral stimulation of the subthalamic nucleus in Parkinson's disease," *Brain*, Vol. 123, pp. 2091–2108 (2000).
9. Alegret, M., C. Junqué, F. Valldeoriola, P. Vendrell, M. Pilleri, J. Rumià, and E. Tolosa, "Effects of bilateral subthalamic stimulation on cognitive function in Parkinson's disease," *Arch. Neurol.*, Vol. 58, pp. 1223–1227 (2001).
10. Schroeder, U., A. Kuehler, A. Hennenlotter, B. Haslinger, V. M. Tronnier, M. Krause, R. Pfister, R. Sprengelmeyer, K. W. Lange, and A. O. Ceballos-Baumann, "Facial expression recognition and subthalamic nucleus stimulation," *J. Neurol. Neurosurg. Psych.*, Vol. 75, pp. 648–650 (2004).
11. Vesper, J., S. Haak, C. Ostertag, and G. Nikkhah, "Subthalamic nucleus deep brain stimulation in elderly patients-analysis of outcome and complications," *BMC Neurol.*, Vol. 7, No. 1, pp. 7–9 (2007).
12. McIntyre, C. C., M. Savasta, B. L. Walter, and J. L. Vitek, "How does deep brain stimulation work? Present understanding and future questions," *J. Clin. Neurophys.*, Vol. 21, No. 1, pp. 40–50 (2004).
13. Butson, C. R., S. E. Cooper, J. M. Henderson, and C. C. McIntyre, "Patient-specific analysis of the volume of tissue activated during Deep Brain Stimulation," *Neuroimage*, Vol. 34, No. 2, pp. 661–670 (2007).
14. Lapicque, L., "Quantitative investigations of electrical nerve excitation treated as polarization. 1907," *Biol. Cybern.*, Vol. 97, No. 5–6, pp. 341–349 (2007).
15. Smith, G., C. Cox, M. Sherman, and J. Rinzel, "Fourier analysis of sinusoidally driven thalamocortical relay neurons and a minimal integrate-and-fire-or-burst model," *J. Neurophysiol.*, Vol. 83, pp. 588–610 (2000).
16. Izhikevich, E., "Which model to use for cortical spiking neuron?" *IEEE Trans. Neural Netw.*, Vol. 15, No. 5, pp. 1063–1070 (2004).
17. Stevens, C. F. and A. M. Zador, "Input synchrony and the irregular firing of cortical neurons," *Nature Neurosci.*, Vol. 1, No. 3, pp. 210–217 (1998).
18. Stein, R. B., "A theoretical analysis of neuronal variability," *Biophys. J.*, Vol. 5, pp. 173–194 (1965).
19. McCormick, D. A. and T. Bal, "Sleep and arousal: Thalamocortical mechanisms," *Ann. Rev. Neurosci.*, Vol. 20, pp. 185–215 (1997).
20. Sherman, S. M., "Tonic and burst firing: Dual modes of thalamocortical relay," *Trends Neurosci.*, Vol. 24, No. 2, pp. 122–126 (2001).
21. Chun, A. L., "Carbon nanofibres on the brain," *Nat. Nanotechnol.*, Vol. 2, No. 8, pp. 465 (2007).
22. Yu, Z., T. E. McKnight, M. Nance Ericson, A. V. Melechko, M. L. Simpson, and B. Morrison III, "Vertically aligned carbon nanofiber arrays record electrophysiological signals from hippocampal slices," *Nano Lett.*, Vol. 7, No. 8, pp. 2188–2195 (2007).